

Electric Field Switching in a Resonant Tunneling Diode Electroabsorption Modulator

José M. Longras Figueiredo, Charles N. Ironside, and Colin R. Stanley

Abstract—The basic mechanism underlying electric field switching produced by a resonant tunneling diode (RTD) is analyzed and the theory compared with experimental results; agreement to within 12% is achieved. The electroabsorption modulator (EAM) device potential of this effect is explored in an optical waveguide configuration. It is shown that a RTD-EAM can provide significant absorption coefficient change, via the Franz-Keldysh effect, at appropriate optical communication wavelengths around 1550 nm and can achieve up to 28-dB optical modulation in a 200- μm active length device. The advantage of the RTD-EAM over the conventional reverse-biased p-n junction EAM, is that the RTD-EAM has, in essence, an integrated electronic amplifier and, therefore, requires considerably less switching power.

Index Terms—Electric field switching, electroabsorption modulation, InGaAlAs waveguide, resonant tunneling diode.

I. INTRODUCTION

WITH the steady improvement of high-precision growth techniques for semiconductor layers, in particular molecular beam epitaxy (MBE), there has been a renaissance in tunneling devices for electronic applications. Compared to previous attempts to produce tunneling devices, high-precision growth now gives much more control over device characteristics which are crucially dependent on layer thickness. Consequently, tunneling devices are now being considered as memory devices [1] and a new logic family has been proposed [2]. Furthermore, it has been demonstrated that III-V semiconductor tunneling devices can be integrated with silicon CMOS technology and that tunneling devices can be driven by CMOS logic levels [3]. The physics and progress in electronic applications of resonant tunneling diodes (RTDs) have recently been reviewed in [4].

Optoelectronics has provided perhaps the most impressive example of high-precision growth for a tunneling device with the invention of the quantum-cascade laser [5] in which population inversion between subbands in quantum wells is produced by carefully engineered tunneling. Simpler optoelectronic device structures essentially based on double-barrier resonant tunneling diodes (DBRTD) have also been used in various applications. These include photodetectors at optical communication wavelengths [6], mid-infrared wavelengths [7] and, closely related to the work presented here, optical modulators [8]–[10].

Manuscript received February 16, 2001; revised August 31, 2001.

J. M. L. Figueiredo is with the Department de Física, Faculdade de Ciências e Tecnologia, Universidade do Algarve, 8000-117 Faro, Portugal (e-mail: jlongras@ualg.pt).

C. N. Ironside and C. R. Stanley are with the Department of Electronics and Electrical Engineering, University of Glasgow, Glasgow G12 8LT, U.K.

Publisher Item Identifier S 0018-9197(01)10052-7.

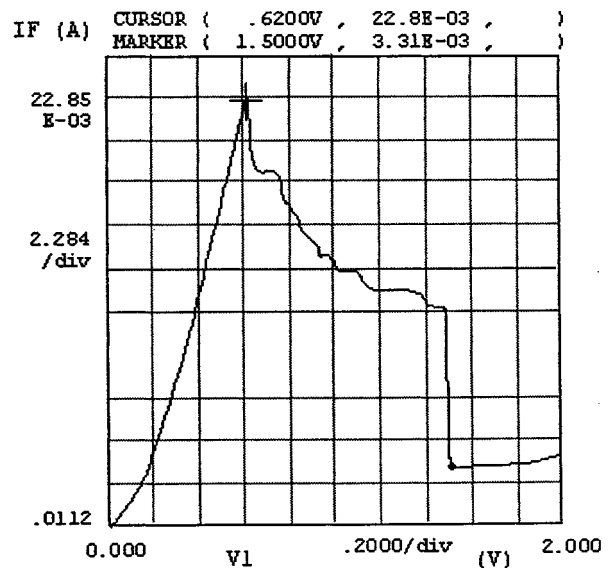


Fig. 1. I - V characteristic of $2\ \mu\text{m} \times 100\ \mu\text{m}$ active area RTD-EAM.

In this paper, we report on the application of a double-barrier RTD to electroabsorption modulator (EAM) devices and, in particular, the electric field switching which is the basis of the operation of the device. We have been investigating this as an alternative to conventional EAM devices which are currently employed in optical communication systems and where the electric field is applied and switched by employing a reversed-biased pin diode. The key advantage of the RTD-EAM over the conventional pin-EAM (for a recent review of conventional pin-EAMs, see [11]) is that the RTD-EAM can provide electrical gain over a wide bandwidth, and thereby achieve a low-drive voltage and high-speed operation.

II. PRINCIPLE OF OPERATION OF THE RTD-EAM

Essentially, the RTD-EAM is a unipolar device which consists of a DBRTD embedded in an optical waveguide. The presence of the DBRTD within the waveguide core introduces high nonlinearities in the current-voltage (I - V) characteristic of the unipolar waveguide. A typical I - V characteristic of a RTD-EAM is shown in Fig. 1 (the physics which gives rise to this type of I - V has been previously explained [4]).

The operation of the RTD-EAM is based on a nonuniform electric field distribution across the waveguide induced by the DBRTD which becomes strongly dependent on the bias voltage. When the current decreases from the peak to the valley, there is an increase of the electric field across the waveguide core. The

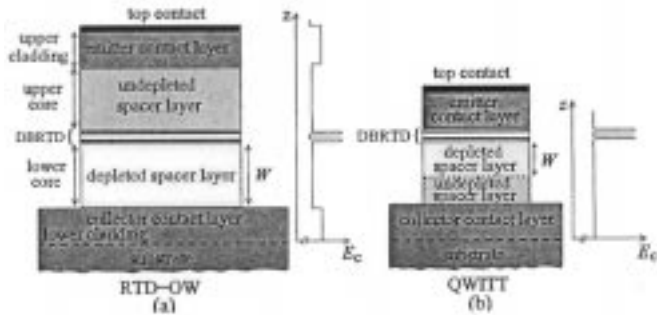


Fig. 2. RTD-EAM and QWITT schematic structures.

electric field enhancement in the depleted spacer layer causes the Franz–Keldysh absorption band-edge to shift to lower energy which is responsible for the electroabsorption effect.

In a conventional EAM, the electric field is applied by reverse biasing a p-n diode that shifts the absorption band-edge of the depleted region to lower energy. The key difference with the RTD-EAM is that the tunneling characteristics of the double-barrier RTD are employed to switch the electric field across the waveguide collector-depleted region. Therefore, a small high-frequency ac signal (<1 V) can induce high-speed switching, producing substantial modulation of light at a photon energy slightly lower than the waveguide band-gap energy.

The RTD-EAM is implemented in a ridged channel unipolar waveguide configuration lying on top of the substrate, Fig. 2(a), and its structure resembles the quantum-well injection transit time (QWITT) diode proposed by Kesan, *et al.* [12], as illustrated in Fig. 2(b). In fact, the RTD-EAM has many similarities to transit-time devices as the tunneling current acts as an injection source to the collector-depleted region [13].

In essence, the RTD-EAM is a DBRTD current switch in series with a resistor, except that the speed of response is limited by the electron transit time across the collector-depleted spacer layer. If one assumes an electron saturation velocity (v_{sat}) of 10^7 cm/s and a depletion region width $W \sim 500$ nm (see Fig. 4), the electron transit time is 5 ps.

The physical mechanism by which the current drop is converted into an electric field enhancement is as follows. When the bound state of the DBRTD quantum well is above or aligned with the emitter conduction band-energy minimum (see diagram of Fig. 3), the electron transmission is high and the carriers can easily tunnel through the bound state with little free-carrier depletion in the collector region. The applied voltage is dropped mainly across the DBRTD and the electric field gradient in the collector spacer layer is small because the spacer layer is not strongly depleted. This corresponds to the transmissive state (on-state) of the modulator (during operation, the RTD-EAM is dc biased slightly below the peak voltage). Once the applied voltage is increased from the peak to the valley, the DBRTD bound state is pulled below the emitter conduction-band energy minimum, as depicted in Fig. 3, and the electrons can no longer tunnel through using the bound state. The current through the device drops, giving rise to an increase of positive space charge in the collector region. A substantial part of the terminal voltage is now dropped across

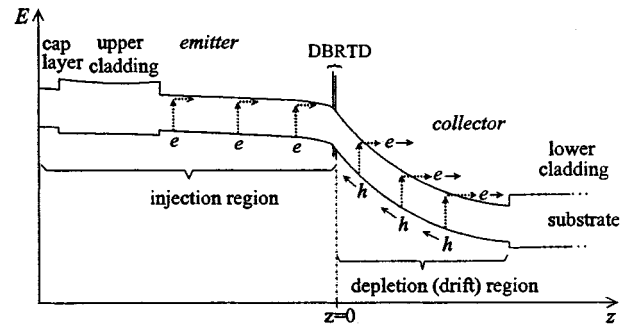


Fig. 3. Schematic diagram of the energy bands in a RTD-EAM at the valley voltage as a function of distance. Upper curve: the lowest conduction band energy. Lower curve: the highest valence band energy.

the collector spacer layer. As a consequence, the magnitude of the electric field in the collector spacer layer increases: this is the nontransmissive state of the modulator. To summarize, the peak-to-valley current drop produces an increase in the magnitude of the electric field across the waveguide core collector region. This causes the broadening of the waveguide absorption band-edge through the Franz–Keldysh effect to longer wavelengths, which in turn leads to an increase of the optical absorption coefficient of photons possessing energy slightly lower the waveguide band-edge energy.

In Fig. 3, we show the energy-band diagram in the RTD-EAM at the valley voltage where the applied voltage is dropped mainly across the depleted region of the waveguide core. To determine the magnitude of the electric field change in the depleted core induced by peak-to-valley switching, the injection region (the emitter and the DBRTD, Fig. 3) is decoupled from the depletion region since its characteristics should not depend strongly on the collector spacer layer [13]. Our analysis follows the QWITT model (see also [14]).

In the analysis, the electric field across the depleted spacer layer (or drift region) is assumed to be high enough to cause the injected electrons to traverse the drift region at a constant saturation velocity, v_{sat} . Quantitatively, the magnitude of the electric field in the drift region as function of position $\mathcal{E}(z)$ at a constant current density J can be obtained from the 1-D Poisson's equation as follows:

$$\frac{\partial \mathcal{E}}{\partial z} = \frac{e}{\epsilon} \left(N_d - \frac{J}{ev_{\text{sat}}} \right) \quad (1)$$

where

- z distance;
- e electronic charge;
- ϵ core permittivity;
- N_d background doping density in the depleted spacer layer.

Integrating, the electric field across the depletion region becomes

$$\mathcal{E}(J; z) = \mathcal{E}_0(J) - \frac{e}{\epsilon} \left(N_d - \frac{J}{ev_{\text{sat}}} \right) \cdot z \quad (2)$$

where $\mathcal{E}_0(J)$ represents the electric field at the injection plane $z = 0$, the boundary between the DBRTD and the depleted

spacer layer (see Fig. 3). The change in voltage across the drift region due to peak-to-valley switching is given by

$$\begin{aligned} \Delta V_d &= \int_0^W [\mathcal{E}(J_v; z) - \mathcal{E}(J_p; z)] dz \\ &= \Delta \mathcal{E}_0 W + \frac{W^2}{2\epsilon v} (J_v - J_p) \end{aligned} \quad (3)$$

where $\Delta \mathcal{E}_0 = \mathcal{E}_{0, J_v} - \mathcal{E}_{0, J_p}$ is the change in the electric field at $z = 0$ between the valley and peak points. The width of the depleted spacer layer W is assumed to remain constant before and after current switching, as is N_d . (W is defined by the thickness of the low doped layer in the collector region of the RTD-EAM.) We can rearrange the above equation to obtain the peak-to-valley electric field enhancement at the injection plane

$$\Delta \mathcal{E}_0 = \frac{\Delta V_d}{W} + \frac{W}{2\epsilon v} \Delta J_{p-v}. \quad (4)$$

The changes in voltage ΔV_d and current $\Delta J_{p-v} = J_p - J_v$ are found from the I - V characteristic of the RTD-EAM.

The analysis of (2) points out an important consideration limiting electric field switching: the background doping of the depleted spacer layer (drift region) N_d must be greater than J_p / ev_{sat} . If this condition is not observed, then the electric field increases with the distance and can exceed the breakdown value. (J_p is essentially determined by the DBRTD structure.) Experimentally, we observed in the InP based RTD-EAM that $N_d = 2 \times 10^{16} \text{ cm}^{-3}$ gave unreliable devices subject to catastrophic breakdown whereas $N_d = 5 \times 10^{16} \text{ cm}^{-3}$ produced reliable devices. Also, doping across the structure, especially in the cladding layers, has to be kept as high as possible to minimize the device series resistance. However, to minimize optical loss due to free carrier losses, it is desirable to keep N_d as small as possible. A compromise between the required electrical and optical properties is needed.

III. WAFER DESIGN AND GROWTH, FABRICATION, AND PACKAGING

The RTD-EAM is a unipolar optical waveguide containing a DBRTD; the DBRTD is employed to switch the electric field developed across the waveguide collector region as described above. The optical waveguide configuration ensures a larger interaction volume between the active region of the device (RTD depletion region) and the optical mode, thereby ensuring a larger modulation depth for a given applied field. The wavelength of operation is set by the band-gap of the material employed in the active region (waveguide core) of the device. Our initial devices used GaAs in the active region (see [8], [9]) and operated at 900 nm, subsequently $\text{In}_{0.53}\text{Ga}_{0.42}\text{Al}_{0.05}\text{As}$ was employed to shift the wavelength of operation to 1550 nm (InGaAlAs was used because it is a convenient semiconductor alloy for MBE growth).

The layer design for the InGaAlAs RTD-EAM device is shown in Fig. 4. The RTD-EAM wafers were grown by MBE in a Varian Gen II system on a InP substrate. The waveguide core was formed by two moderately doped (Si: $5 \times 10^{16} \text{ cm}^{-3}$) $\text{In}_{0.53}\text{Ga}_{0.42}\text{Al}_{0.05}\text{As}$ layers 500-nm thick (absorption band edge around 1520 nm and refractive index of 3.56) each side

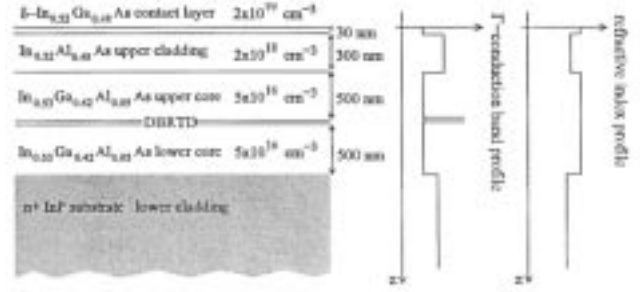


Fig. 4. InGaAlAs-InP wafer structure, Γ -valley, and refractive index profiles.

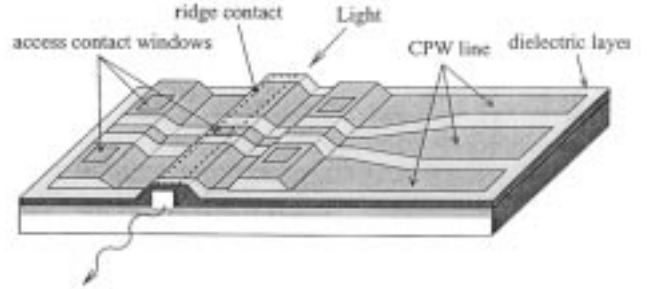


Fig. 5. Schematic of the RTD-EAM.

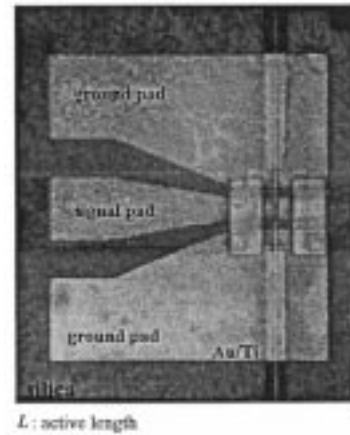


Fig. 6. Top view of a RTD-EAM die ($430 \mu\text{m} \times 500 \mu\text{m}$ with $L = 100 \mu\text{m}$), showing the CPW contact-pad/transmission line.

of the DBRTD (2-nm-thick AlAs barriers and 6-nm-thick $\text{In}_{0.53}\text{Ga}_{0.47}\text{As}$ quantum well). The upper cladding layer of the optical waveguide consisted of a 300-nm $\text{In}_{0.52}\text{Al}_{0.48}\text{As}$ layer heavily doped (Si: $2 \times 10^{18} \text{ cm}^{-3}$). The contact layer was a $\text{In}_{0.53}\text{Ga}_{0.47}\text{As}$ layer δ -doped for the formation of nonalloyed Au-Ge-Ni ohmic contacts.

Ridge waveguides (2–6- μm wide) and large-area mesas on each side of the ridges were fabricated by wet-etching. Ohmic contacts (100–400- μm long) were deposited on top of the ridges and mesas. The waveguide width and the ohmic contact length define the device active area. A SiO_2 layer was deposited, and access contact windows were etched on the silica over the ridge and the mesa electrodes (Fig. 5), allowing contact to be made through high-frequency bonding pads (coplanar waveguide transmission line, CPW). Fig. 5 shows the layout of the RTD-EAM chip and Fig. 6 is an annotated photograph showing the top view of a finished RTD-EAM die.

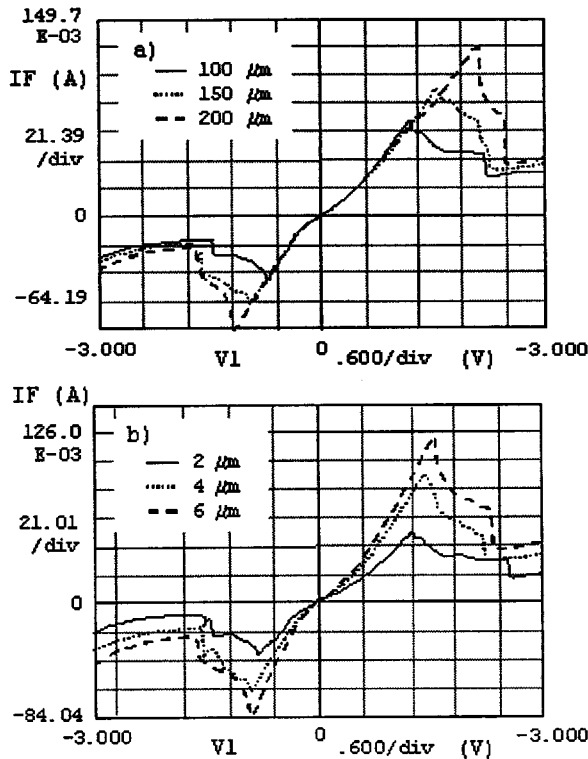


Fig. 7. RTD-EAM I - V characteristics with: (a) active length 100, 150, and 200 μm and 4- μm wide and (b) width 2, 4, and 6 μm and 150- μm long, as parameter.

After cleaving, the devices were die bonded on packages allowing light to be coupled into the waveguide by a microscope objective end-fire arrangement. The details of the fabrication procedure and device packaging can be found in [14].

IV. RESULTS

Here we report on the electrical and the optical characterization of the InGaAlAs-InP RTD-EAM. The electrical characterization was concerned with dc measurements of the I - V curve and the optical characterization was concerned with low-frequency modulation and background loss measurements.

The dc electrical characteristics of the packaged devices were measured using a HP 4145 parametric analyzer. Fig. 7 shows two typical I - V curves for devices of different active lengths and widths. The peak voltage rises as the active area increases. Typical $4 \times 200 \mu\text{m}^2$ active area RTD-EAMs show peak current densities up to $18 \text{ kA}\cdot\text{cm}^{-2}$ and peak-to-valley current ratios of around 4, with valley-to-peak voltage difference (ΔV_{v-p}) of 0.8 V and peak-to-valley current density change up to $\Delta J_{p-v} = 13 \text{ kA}\cdot\text{cm}^{-2}$. Some devices showed larger peak-to-valley current ratios and up to 7 could be achieved (see Fig. 1).

An interesting feature of the I - V curves is that they are not completely anti-symmetric, the peak voltage in the reverse region is smaller in magnitude compared to the positive voltage side and, indeed, it was frequently the case that devices operated in the forward voltage showed catastrophic electrical breakdown. This behavior may be related to the unsymmetric nature of the layer structure and the different electrical characteristics of the InAlAs alloy, forming the upper cladding, compared to

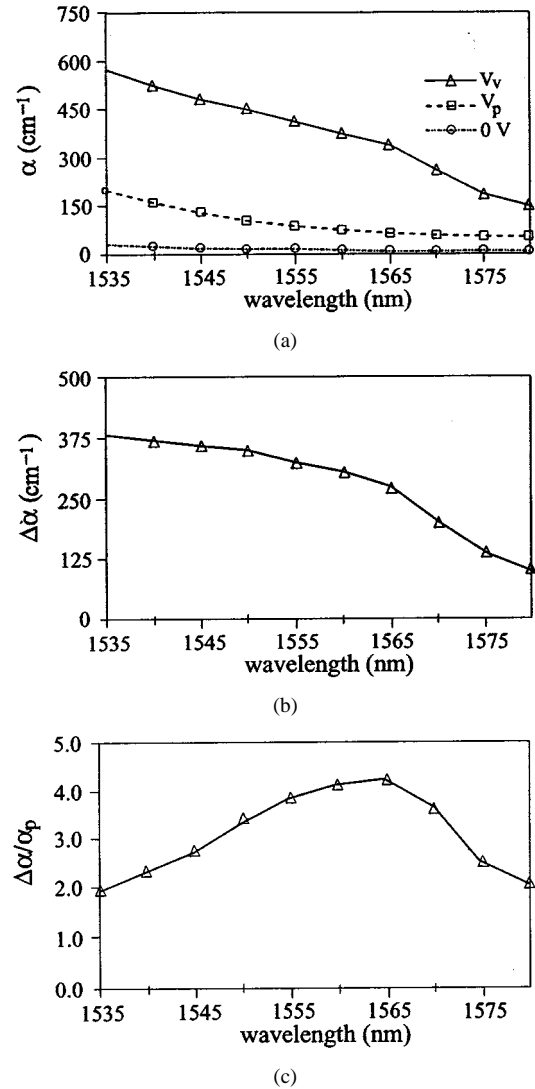


Fig. 8. Typical RTD-EAM absorption spectra characterization. (a) Absorption, α at zero, at the peak and at the valley voltages. (b) Absorption change, $\Delta\alpha = \alpha_v - \alpha_p$, where α_v and α_p represent the absorption at the valley and peak points, respectively. (c) Change in the absorption coefficient over the absorption coefficient at peak voltage $\Delta\alpha/\alpha_p$.

the InP substrate which acts as the lower cladding. In the optical experiments described below, devices were operated in the negative voltage side of the I - V curve, i.e., electrons flowing toward the substrate.

Optical characterization of the InGaAlAs RTD-EAMs employed a diode laser, tunable in the wavelength range of 1480–1580 nm. End-fire and fiber coupling into the semiconductor waveguide were employed. The waveguide was not single mode but it was possible to excite individual modes with a single mode fiber. By tuning the laser and measuring the throughput, the waveguide transmission spectra was obtained. The Fabry-Perot etalon method was employed to calibrate the spectra by measuring the loss at a particular wavelength. For zero applied field, the absorption coefficient at 1565 nm was found to be 8.2 cm^{-1} . The change in the absorption spectrum was measured at various points in the I - V curve of the RTD-EAM, as shown in Fig. 8(a). The absorption change induced by peak-to-valley switching $\Delta\alpha = \alpha_v - \alpha_p$ is presented in Fig. 8(b). Fig. 8(c)

summarizes the results of these experiments, showing the degree of electroabsorption characterized by the change in optical absorption coefficient induced by the peak-to-valley transition $\Delta\alpha$, over the absorption coefficient at the peak bias α_p , $\Delta\alpha/\alpha_p$.

Preliminary electroabsorption modulation results have been previously reported [10]; in summary, devices with a $4 \times 200 \mu\text{m}^2$ active area showing the highest peak-to-valley current ratio and largest ΔV_{v-p} , when dc biased to the optimum operating point, had a maximum modulation depth of 28 dB at around 1565 nm [10]. Typical $4 \times 200 \mu\text{m}^2$ active area devices showed a modulation depth of around 20 dB in the wavelength range 1560–1567 nm, with propagation loss in the transmissive state estimated to be ~ 5 dB [14]. The quiescent power required to bias the device in the on-state (near the switching point V_p), is around 30 mW. Furthermore, in collaboration with other groups [15], we have shown that with these devices, it is possible to achieve a modulation of 5 dB for a voltage change of 1 mV. We estimate that 10 dB of modulation can be achieved for a power of a few milliwatts.

V. COMPARISON WITH THEORY

Considering the $4 \times 200 \mu\text{m}^2$ active area InGaAlAs RTD-EAM devices with measured values of ΔV_{v-p} around 0.8 V and $\Delta J_{p-v} = 13 \text{ kAcm}^{-2}$, taking $\epsilon = 14\epsilon_0$, $v_{\text{sat}} = 1 \times 10^7 \text{ cm/s}$ [16], we find an electric field enhancement $\Delta\mathcal{E}_0 = 43 \text{ kV/cm}$, as in (4) (where W corresponds to the width of the low doped layer on the collector side of the RTD; in this present structure, 500 nm).

In the calculation of the absorption band-edge shift, a uniform electric field across the depleted region is assumed, and any shift due to thermal effects as a consequence of the current flow and the peak voltage is neglected. Assuming $\mathcal{E}_0(J_v) \gg \mathcal{E}_0(J_p)$, $\Delta\mathcal{E}_0 \cong \mathcal{E}_0(J_v)$, the shift in the InGaAlAs waveguide transmission spectrum due to electric field enhancement as a result of the Franz–Keldysh effect is given approximately by [8]

$$\Delta\lambda_g \cong \frac{\lambda_g^2}{hc} \left(\frac{e^2 h^2}{8\pi^2 m_r} \right)^{1/3} \Delta\mathcal{E}^{2/3} \quad (5)$$

where

- m_r electron-hole system reduced effective mass;
- h Planck's constant;
- c light velocity;
- e electron charge;
- λ_g wavelength corresponding to the waveguide transmission edge at zero bias.

To calculate the band-edge shift, we use the band-gap wavelength of $\text{In}_{0.53}\text{Ga}_{0.42}\text{Al}_{0.05}\text{As}$, $\lambda_g = 1520 \text{ nm}$, and the following effective masses values (appropriate for the $\text{In}_{0.53}\text{Ga}_{0.42}\text{Al}_{0.05}\text{As}$ alloy), $m_e = 0.046m_0$ and $m_{hh} = 0.5m_0$ (only the lowest electron-to-heavy-hole transitions are considered). From the above equation, we obtain $\Delta\lambda_g = 46 \text{ nm}$ compared to the observed value $\Delta\lambda_g = 43 \text{ nm}$, indicating an actual electric field of 38 kV/cm. This provides evidence that (4) predicts, as a first approximation, the magnitude of the electric field enhancement to 12% accuracy. We,

therefore, conclude that our model gives a good estimate of the switched electric field $\Delta\mathcal{E}_0$, and thereby the band-edge shift can be approximately calculated.

The RTD has been described as the fastest purely electronic device and oscillation at up to 712 GHz has been reported from an RTD device [17]. Streak camera studies of our GaAs RTD-EAM demonstrated 30-ps pulses of light and self-oscillation at up to 16 GHz, which analysis of the design suggested was limited by the electronic packaging [9], [14]. A similar streak camera investigation of the InAlGaAs RTD-EAM high-speed characteristics could not be undertaken because of the low radiant sensitivity of the streak tube at 1550 nm. The next stage in the development of the InAlGaAs RTD-EAM will be to employ other types of detectors for an investigation of its high-speed operation. These studies will be undertaken after further optimization of the design of the device and the package.

VI. CONCLUSION

We have presented a study of the basic mechanism of electric field switching with a RTD and have demonstrated how this electric field switching can be employed in an electroabsorption modulator device configuration to obtain optical modulation at 1550 nm. The analysis of the electric field switching is based on the QWITT model [12], [13] which explicitly takes account of the electric field across the depleted spacer layer. In the RTD-EAM, it is the band-edge shift in the depleted spacer layer, via the Franz–Keldysh effect, which gives rise to the observed optical modulation; the optical waveguide configuration is employed to confine light in the depleted spacer layer. The value of the switched electric field was deduced from the absorption band-edge shift and the model was shown to give an estimate to within 12% of this switched electric field. The model assumes a uniform electric field across the depleted region but it could be further refined by taking account of the graded electric field across the depleted spacer layer.

The change in the optical absorption coefficient induced by the peak-to-valley transition over the absorption coefficient at the peak current $\Delta\alpha/\alpha_p$ associated with the switch in electric field shows a maximum value of 4 at a wavelength of 1565 nm. This effect was employed (combined with an applied voltage swing slightly larger than ΔV_{v-p}) to obtain a maximum modulation of 28 dB at 1565 nm in a device with an active region length of 200 μm . The magnitude of the switched electric field in the RTD-EAM was found to be around $\Delta\mathcal{E}_0 = 43 \text{ kV/cm}$ which compared with $>100 \text{ kV/cm}$ obtainable with a pin-EAM [11].

The insertion loss due to the absorption coefficient in the transmissive state α_p is a material property which depends on the electric field value at the on-state operating voltage [11]. The insertion loss caused by the waveguide-fiber mode mismatch and the reflections at the facets have the same magnitude as conventional EAMs. The reduction in the on-state voltage and the improvement of the guiding characteristics of the waveguide, which we believe can be achieved in an optimized device, will lead to a smaller α_p , decreasing the insertion loss to levels similar to those for conventional EAMs.

The expected quiescent power dissipation of 30 mW in the on-state in typical applications can be regarded as a dc power supply. The conventional EAM chip requires less quiescent drive power (it depends on the transmissive state bias electric field). However, it needs a RF amplifier to drive it. The RTD-EAM provides on-chip electrical amplification which can be employed to substantially reduce the power required from the high-frequency (RF) applied data signal and thereby remove the requirement of an external rf amplifier. In addition, the electrical characteristics of the RTD are well suited for digital modulation and can be combined with recent developments in RTDs for purely electronic applications to develop a new high-speed digital technology. Driving many of these developments is the intrinsic high speed of the tunneling process which has already been demonstrated to operate at over 700 GHz and could be harnessed in a combination optoelectronic and electronic device to provide the high-speed communication, memory, and processing required by the next generation of information technology. However, it should also be noted that the operating parameters of tunneling devices are sensitive to device dimensions on a nanometer scale and even with the steady improvement in epitaxial growth techniques there are still significant challenges ahead in making this a manufacturable technology [18].

REFERENCES

- [1] J. P. A. Van Der Wagt, "Tunneling based SRAM," *Proc. IEEE*, vol. 87, pp. 571–595, 1999.
- [2] R. H. Mathews, J. P. Sage, T. C. L. G. Sollner, S. D. Calawa, C. Chen, L. J. Mahoney, P. A. Maki, and K. M. Molvar, "A new RTD-FET logic family," *Proc. IEEE*, vol. 87, pp. 596–605, 1999.
- [3] J. I. Bergman, J. Chang, Y. Joo, B. Matinpour, J. Lasker, N. M. Jornerst, M. A. Brooke, B. Brar, and E. Beam, III, "RTD/CMOS nanoelectronic circuits: Thin-film InP-based resonant tunneling diodes integrated with CMOS circuits," *IEEE Electron Device Lett.*, vol. 20, pp. 119–122, 1999.
- [4] H. Mizuta and T. Tanoue, *Physics and Applications of Resonant Tunneling Diodes*. Cambridge, U.K.: Cambridge Univ. Press, 1995.
- [5] J. Faist, F. Capasso, D. L. Sivco, C. Satori, A. L. Hutchinson, and A. Y. Cho, "Quantum cascade laser," *Science*, vol. 264, pp. 533–556, 1994.
- [6] T. S. Moise, Y.-C. Kao, C. L. Goldsmith, C. L. Schow, and J. C. Campbell, "High-speed resonant tunneling diodes photodiodes with low switching energy," *IEEE Photon. Technol. Lett.*, vol. 9, pp. 803–805, 1997.
- [7] C. Mermelstein and A. Sa'ar, "Intersubband photocurrent from double barrier resonant tunneling structures," *Superlatt. Microstruct.*, vol. 19, pp. 375–382, 1996.
- [8] S. G. McMeekin, M. R. S. Taylor, B. Vögele, C. R. Stanley, and C. N. Ironside, "Franz-Keldysh effect in optical waveguide containing a resonant tunneling diode," *Appl. Phys. Lett.*, vol. 65, pp. 1076–1078, 1994.
- [9] J. M. L. Figueiredo, C. R. Stanley, A. R. Boyd, C. N. Ironside, S. G. McMeekin, and A. M. P. Leite, "Optical modulation in a resonant tunneling relaxation oscillator," *Appl. Phys. Lett.*, vol. 74, pp. 1197–1199, 1999.
- [10] —, "Optical modulation at around 1550 nm in InGaAlAs optical waveguide containing a InGaAs/AlAs resonant tunneling diode," *Appl. Phys. Lett.*, vol. 75, pp. 3443–3445, 1999.
- [11] K. Wakita, *Semiconductor Optical Modulators*. Norwell, MA: Kluwer, 1998.
- [12] V. P. Kesan, D. P. Neikirk, B. G. Streetman, and P. A. Blakey, "The influence of transit-time effects on the optimum design and maximum oscillation frequency of quantum well oscillators," *IEEE Trans. Electron Devices*, vol. 35, pp. 405–413, 1988.
- [13] S. Yngvesson, *Microwave Semiconductor Devices*. Norwell, MA: Kluwer, 1991.
- [14] J. M. L. Figueiredo, "Optoelectronic properties of resonant tunnelling diodes," Ph.D. dissertation, Univ. of Porto, Porto, Portugal, 2000.
- [15] J. M. L. Figueiredo, A. M. P. Leite, C. N. Ironside, C. R. Stanley, S. G. McMeekin, K. Bouris, and D. G. Moodie, "Resonant tunneling diode electroabsorption waveguide modulator operating at around 1550 nm," in *Proc. Tech. Dig. Conf. Laser Electro-Optics (CLEO 2000)*, 2000, pp. 596–597.
- [16] A. F. J. Levi, "Nonequilibrium electron transport in heterojunction bipolar transistors," in *Growth, Processing and Applications InP HBTs*, B. Jalali and S. J. Pearton, Eds. Norwood, MA: Artech, 1995, ch. 4.
- [17] E. R. Brown, J. R. Soderstrom, C. D. Parker, L. J. Mahoney, K. M. Molvar, and T. C. McGill, "Oscillations up to 712 GHz in InAs/AlSb resonant-tunneling diodes," *Appl. Phys. Lett.*, vol. 85, pp. 2291–2293, 1991.
- [18] V. A. Wilkinson, M. J. Kelly, and M. Carr, "Tunnel devices are not yet manufacturable," *Semiconductor Sci. Technol.*, vol. 12, pp. 91–99, 1997.

José M. Longras Figueiredo was born in Barcelos, Portugal. He received the B.Sc. degree in physics (optics and electronics) in 1991 from the University of Porto, Porto, Portugal (his final year project on holographic optical elements aberration correction with an intermediate computer-generated hologram was completed under the ERAMUS Programme at the Vrije Universiteit Brussels) and the M.Sc. degree in optoelectronics and lasers in 1995 (with a thesis on wavelength-division multiplexing integrated optical devices).

From 1995 to 1999, he was with the Department of Electronics and Electrical Engineering, University of Glasgow, Glasgow, U.K., as a Ph.D. student working on the optoelectronic properties of resonant tunneling diodes. His current research interests include the design and characterization of optoelectronic devices.

Charles N. Ironside was born in Aberdeen, Scotland, U.K. He received the B.Sc. degree (first-class honors) in physics in 1974, and the Ph.D. degree in 1978, both from Heriot-Watt University, Edinburgh, U.K. His Ph.D. work involved the Spin-Flip Raman Laser, a type of tunable semiconductor laser.

From 1978 to 1984, he was a post-doctoral Research Assistant at the University of Oxford, Oxford, U.K., first with the Inorganic Chemistry Department, working on time-resolved spectroscopy of solids and energy-transfer mechanisms between luminescent ions, and then with the Clarendon Laboratory, working on time-resolved spectroscopy of solids on a picosecond timescale and ultrafast effects in semiconductors. In 1984, he moved to the Department of Electronics and Electrical Engineering, University of Glasgow, Glasgow, U.K. He has published more than 150 research papers. His current research interests include ultrafast all-optical switching in semiconductor waveguides, monolithic modelocking of semiconductor lasers, and ultrafast optoelectronic modulators employing resonant tunneling diodes and quantum-cascade lasers.

Colin R. Stanley was born in Tunbridge Wells, U.K., in 1945. He received the first-class honors degree in electronic engineering from the University of Sheffield, Sheffield, U.K., in 1966, and the Ph.D. degree (for research into the nonlinear optical properties of tellurium) from the University of Southampton, Southampton, U.K., in 1970.

From 1970 to 1972, he was an I.C.I. Research Fellow at the University of Southampton, continuing work on optical parametric amplifiers and oscillators. He spent part of 1971 at the Centre Nationale d'Etudes des Telecommunications, Bagneux, Paris, France, as a Visiting Scientist. He joined the Department of Electronics and Electrical Engineering, University of Glasgow, Glasgow, Scotland, in 1972 as a Research Fellow, and was subsequently appointed Lecturer (1974), Senior Lecturer (1982), Reader (1989), and Titular Professor (1992). He was a Visiting Scientist at Cornell University, Ithaca, NY, during 1982, and spent six months during 1997–1998 on industrial secondment with Motorola, East Kilbride, under a scheme financed by the Royal Academy of Engineering. He has been author or co-author of over 90 papers on MBE and related topics.

Dr. Stanley is a member of the EPSRC Functional Materials College, the Institution of Electrical Engineers, and the Institute of Physics.